

A cell-level model of pharmacodynamics-mediated drug disposition

Wojciech Krzyzanski¹ · John M. Harrold² · Liviawati S. Wu² · Juan Jose Perez-Ruixo^{2,3}

Received: 10 May 2016 / Accepted: 2 September 2016 / Published online: 9 September 2016
© Springer Science+Business Media New York 2016

Abstract We aimed to develop a cell-level pharmacodynamics-mediated drug disposition (PDMDD) model to analyze in vivo systems where the PD response to a drug has an appreciable effect on the pharmacokinetics (PK). An existing cellular level model of PD stimulation was combined with the standard target-mediated drug disposition (TMDD) model and the resulting model structure was parametrically identifiable from typical in vivo PK and PD data. The PD model of the cell population was controlled by the production rate k_{in} and elimination rate k_{out} which could be stimulated or inhibited by the number of bound receptors on a single cell. Simulations were performed to assess the impact of single and repeated dosing on the total drug clearance. The clinical utility of the cell-level PDMDD model was demonstrated by fitting published data on the stimulatory effects of filgrastim on absolute neutrophil counts in healthy subjects. We postulated repeated dosing as a means of detecting and quantifying PDMDD as a single dose might not be sufficient to elicit the cellular response capable of altering the receptor pool to visibly affect drug disposition. In the absence of any PD effect, the model reduces down to the standard TMDD model. The applications of this model can be readily extended to include chemotherapy-induced cytopenias affecting

clearance of endogenous hematopoietic growth factors, different monoclonal antibodies and immunogenicity effects on PK.

Keywords Target-mediated drug disposition · Cell populations · Filgrastim · Absolute neutrophil count

Introduction

Target-mediated drug disposition (TMDD) occurs when a drug binds with high affinity to pharmacological targets (e.g., receptors) such that this interaction is reflected in the pharmacokinetic (PK) characteristics of the drugs [1]. If the binding elicits a pharmacological effect that in turn affects the size of the target pool which leads to appreciable changes in the drug disposition over time, then this system is said to exhibit pharmacodynamics-mediated drug disposition (PDMDD) [2]. The most prevalent systems exhibiting PDMDD are populations of cells expressing membrane-bound receptors, which are activated by the drug and result in changes in the cellular concentration, subsequently changing the receptor pool size.

The concept of the PDMDD has been established for hematopoietic growth factors. The clearance of the agonists of the granulocyte colony stimulating factor (G-CSF) receptor, filgrastim and pegfilgrastim, changes over time with the changing absolute neutrophil count (ANC) in response to treatment [3]. Consequently, an increase in ANC upon multiple doses coincides with a decrease of filgrastim area under the curve between the doses. A decrease of ANC in the chemotherapy induced neutropenia correlates with an increase in the level of the endogenous G-CSF of cancer patients [4]. Similar behavior has been observed when pegfilgrastim was administered to

✉ John M. Harrold
jharrold@amgen.com

¹ Department of Pharmaceutical Sciences, University at Buffalo, Buffalo, USA

² Clinical Pharmacology, Modeling, and Simulation, Amgen Inc., One Amgen Center Dr, Thousand Oaks, CA 91320, USA

³ Present Address: Janssen Research & Development, Beerse, Antwerp, Belgium

nonhuman primates both with and without radiation exposure. At equivalent doses, pegfilgrastim was shown to have a higher exposure when administered to irradiated animals experiencing neutropenia versus non-irradiated animals [5]. In another example, the clearance of c-Mpl receptor agonists has been shown to be related to platelet counts. Escalating intravenous (IV) bolus doses of romiplostim administered to healthy subjects, animals and patients resulted in decreased clearances and increased peaks of platelets count [6, 7]. Also, an inverse relationship was reported between levels of endogenous thrombopoietin and platelet nadir in patients with acute myeloid leukemia undergoing dose intensive chemotherapy [8]. Furthermore, the clearance of erythropoiesis stimulating agent, epoetin α , increases after multiple doses in healthy subjects [9, 10].

The PDMDD phenomenon has also been reported for some monoclonal antibodies. For instance, peaks and troughs of plasma concentration of a monoclonal antibody alemtuzumab targeting the CD52 antigen, a glycoprotein found on the cell surface lymphocytes and monocytes, increase following multiple doses in patients with chronic lymphocytic leukemia with a parallel decrease in the white cell blood counts [11]. Tocilizumab is a humanized anti-interleukin-6 (IL-6) receptor monoclonal antibody that has demonstrated efficacy in the treatment of rheumatoid arthritis (RA). IL-6 receptor (IL-6R) is present as soluble and membrane bound species expressed on cells of the immune system such as neutrophils and lymphocytes as well as on hematopoietic precursors. Tocilizumab has been shown to exhibit PDMDD and cause the suppression of neutrophils, white blood cells, and platelet counts following multiple infusions in RA patients [12]. In addition, the development of immune response and the generation of antidrug antibodies following the administration of monoclonal antibodies such as adalimumab or infliximab generate an increase of drug clearance that is consistent with the PDMDD concept [13].

PK/PD models of systems exhibiting PDMDD must account for the nonlinear concentration- and nonstationary clearance, in addition to the other relevant nonlinear PK/PD processes. Models applying the Michaelis–Menten mechanism for saturable clearance often relate the V_{\max} term to the cell count response [11, 14]. This allows one to correlate the drug clearance with PDs. Also, for models employing TMDD equations, it is common to assume that the total receptors are proportional to the cell count response [2, 15]. As a result, the binding capacity of the receptor pool is directly determined by the cell number expressing the receptors, which is the key feature of the PDMDD. Therefore, the kinetics of the total receptor pool is entirely controlled by the cell dynamics, and ignores the contributions of the receptor synthesis, degradation, and internalization of the drug–receptor complex [16, 17].

These simplifications are useful to develop explanatory models, however, they limit the predictive power because the dynamic interaction between the PK and PD is not intrinsically accounted for. Therefore, PDMDD models require simultaneous analysis of the PK and PD data, and the model structure must include the intrinsic interaction between PK and PD [2].

Cell-level models have been developed to describe receptor binding, intracellular trafficking, and degradation [18]. The drug–receptor complex is internalized via endocytosis and embedded in the lysosome. Inside the lysosome, the drug dissociates from the receptor and is sorted for recycling or degradation. The recycled drug is secreted back into the extracellular matrix as intact ligand. The cell-level model was also linked with a PD model of the cell population to account for the receptor-mediated drug clearance [19, 20]. Such models can be considered PDMDD models according to the definition presented above. Cell-level models contain a number of parameters describing intracellular processes, which can be only identified from *in vitro* data. These cell-level models become problematic from an identifiability perspective because *in vivo* clinical data typically includes only drug plasma concentrations and cellular responses.

Our objective was to incorporate the salient aspects of the cell-level model developed by Sarkar and Lauffenburger [19] into the traditional TMDD model developed by Mager and Jusko [21] such that PD impacts on exposure could be fully characterized. A structurally parsimonious cellular-level PDMDD model was developed such that the parameters impacting clearance and efficacy could be identifiable from typical *in vivo* PK/PD data. To demonstrate the utility of this model in a clinical setting, the cell-level PDMDD model was used to describe published data on the stimulatory effect of filgrastim on ANC in healthy subjects.

Methods

Model structure

To account for the PDMDD we modify the general TMDD model [21] by partitioning the free (R) and bound (B) receptor pools into the single cell and the cell population components as shown in Fig. 1. The major assumption is that the number of free and bound receptors in the central compartment is the product of the number of free (r) and bound (b) receptors on a single cell and the number of cells (N), yielding the following equations for the receptor concentrations:

$$R = \xi \cdot r \cdot N/V_c \quad \text{and} \quad B = \zeta \cdot b \cdot N/V_c, \quad (1)$$

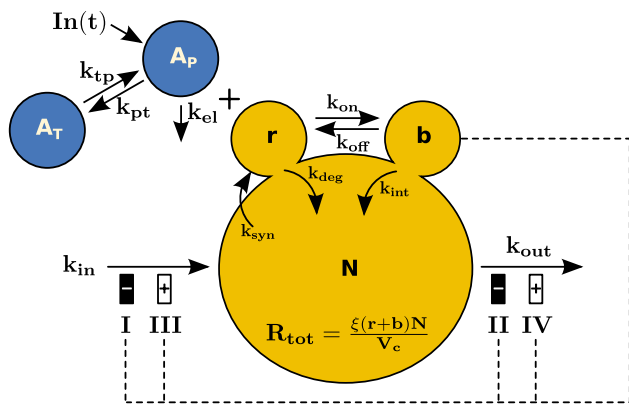


Fig. 1 Schematic diagram for a general cell-level PDMDD model. N represents the population of cells with free (r) and bound (b) receptors on a single cell. The free receptors are synthesized (k_{syn}) and degraded (k_{deg}). They bind to drug molecules (k_{on}) and form bound receptors. The bound receptors dissociate (k_{off}) yielding free bound receptors and free drug, and are internalized (k_{int}). The bound receptors control the production (k_{in}) and elimination (k_{out}) of the cells. The *open* (+) and *solid* (−) symbols represent stimulation and inhibition, respectively. The compartment A_P is the drug amount in available for binding to the cell receptors (e.g., drug in the plasma). The compartment A_T is the amount of drug not available for binding the cells (e.g., peripheral tissue). The drug can be eliminated (k_{el}) or distributed to and from A_T (k_{tp} and k_{pt}). The $In(t)$ is the input of the drug into the central compartment A_P accounting for an arbitrary administration route

where V_c is the volume of central compartments and ξ is the scaling factor converting the units of cell cellular concentration to nanomolar amounts. The free drug part of the TMDD model remains the same.

Pharmacokinetic model

The relationships in Eq. (1) can be incorporated to the equations for the amount of free drug in the central (A_P) and peripheral (A_T) compartments as defined by the general TMDD model [21]:

$$\frac{dA_P}{dt} = In(t) - (k_{el} + k_{pt}) \cdot A_P + k_{tp} \cdot A_T - (k_{on} \cdot r \cdot A_P / V_c - k_{off} \cdot b) \cdot \xi \cdot N, \tag{2}$$

$$\frac{dA_T}{dt} = k_{pt} \cdot A_P - k_{tp} \cdot A_T, \tag{3}$$

where the free drug concentration in the central compartment, C , is

$$C = \frac{A_P}{V_c}. \tag{4}$$

Cell-level model

To describe the turnover and drug binding by receptors expressed on a single cell, the approach applied previously

by Shankaran et al. was adopted [22]. Free receptors expressed on the cell membrane are synthesized at the zero-order rate k_{syn} and degraded at the first-order rate k_{deg} . Receptors bind drug molecules at the second-order rate k_{on} forming the drug–receptor complexes (bound receptors) that dissociate at the first-order rate k_{off} . The bound receptors are internalized via endocytosis at the first-order rate k_{int} and they are subsequently degraded in the cellular endosomes. For simplicity, we assume that there is no recycling of the drug–receptor complex:

$$\frac{dr}{dt} = k_{syn} - k_{deg} \cdot r - k_{on} \cdot r \cdot C + k_{off} \cdot b, \tag{5}$$

$$\frac{db}{dt} = k_{on} \cdot r \cdot C - (k_{off} + k_{int}) \cdot b. \tag{6}$$

Pharmacodynamic model

Similar to Sarkar et al. we assume that the cell population is controlled by the production rate k_{in} and elimination rate k_{out} each of which can be stimulated or inhibited by the drug [19]. However, instead of the drug concentration C as a driver of the effect, we propose that the number of bound receptors/cell represent the pharmacological stimulus, which is further transduced to elicit the effect on turnover rate of the cell population:

$$\frac{dN}{dt} = k_{in} \cdot (1 + H_{in}(b)) - k_{out} \cdot (1 + H_{out}(b)) \cdot N, \tag{7}$$

where four drug effect functions are considered according to the basic mechanisms for indirect response models [23]:

$$(H_{in}(b), H_{out}(b)) = \begin{cases} \left(\frac{S_{max}b}{Sb_{50} + b}, 0 \right), \\ \left(-\frac{I_{max}b}{Ib_{50} + b}, 0 \right), \\ \left(0, \frac{S_{max}b}{Sb_{50} + b} \right), \\ \left(0, -\frac{I_{max}b}{Ib_{50} + b} \right), \end{cases} \tag{8}$$

where $S_{max} > 0$ and $0 \leq I_{max} \leq 1$ denote the maximal effects and Sb_{50} and Ib_{50} are the number of bound receptor/cell eliciting half of the maximal stimulatory or inhibitory effect, respectively.

Initial conditions

It is assumed that drug is input to the central compartment by means of the input function $In(t)$, and, initially, there is no drug present in the system.

$$A(0) = 0 \quad \text{and} \quad A_T(0) = 0. \tag{9}$$

We also assume that, prior to the drug administration; the system was at the steady-state with a nominal number of cells, free and bound receptors:

$$N(0) = \frac{k_{in}}{k_{out}}, \quad r(0) = \frac{k_{syn}}{k_{deg}}, \quad \text{and} \quad b(0) = 0. \quad (10)$$

Simulations

A series of simulations has been performed to explore free drug concentrations in the plasma and receptor numbers on a single cell after single dose administration, and the cellular response on the drug clearance following repeated doses.

Single and repeated doses

The impact of a single IV bolus dose versus repeated daily IV bolus doses of 10,000 pmol was considered for each of the models described by (4).

$$In(t) = Dose_{IV} \cdot \delta(t) \quad \text{or} \quad In(t) = \sum_{i=1}^n Dose_{IV} \cdot \delta(t - t_i), \quad (11)$$

where $\delta(t)$ is the Dirac delta function and $t_i = 1, \dots, n$ are the dosing times. Single and repeated dosing was considered because the cellular response to stimulation typically occurs on a timescale which is much longer than that of the

drug kinetics. As such, the number of cells (N) accumulate following repeated doses, which has an impact on the receptor pool (R), and consequently, on the clearance of the drug. To characterize the interactions of these aspects of the system, time course of the free drug concentration, cellular response, as well as the total drug clearance were simulated and compared to the scenario where the drug has no PD effect.

Model parameters

In order to focus on the PDMDD phenomena being studied a single set of parameters were selected to exemplify the studied features for all of the cases in Fig. 1. These parameters, summarized in Table 1, were used to perform simulations. The system was constructed in Ubiquity [24] and simulations were performed in Matlab (2012b, The Mathworks, Natick, MA).

Case study

Data from two previously published filgrastim Studies 930240 [14] and 91770 [25] were selected to study the PDMDD phenomena. Filgrastim is a G-CSF analog that stimulates neutrophil synthesis and maturation by binding to the G-CSF receptor. For each study, filgrastim was administered to healthy volunteers and both PK and PD (ANC) measures were recorded. Data from Study 930240 was selected to characterize the PK/PD relationship

Table 1 Parameter values used for simulations of the time courses of the model variables shown in Figs. 2 and 3

Parameter (unit)	Definition	Value
$Dose_{IV}$ (pmol)	IV bolus dose	10,000
k_{el} (h^{-1})	First-order rate constant for systemic elimination of the drug	0.53
V_c (L)	Volume of the central compartment	1.81
k_{pt} (h^{-1})	First-order rate constant for drug distribution to the tissue space	0.1
k_{tp} (h^{-1})	First-order rate constant for drug distribution from the tissue space	0.2
k_{in} (10^9 cells/h)	Zero-order production rate constant for the cell population	0.3
k_{out} (h^{-1})	First-order elimination rate constant for the cell population	0.02
k_{syn} (receptors/cell/h)	Zero-order synthesis rate constant for free receptors expressed on the cell membrane	15,000
k_{deg} (h^{-1})	First-order degradation rate constant for free receptors expressed on the cell membrane	3.54
k_{on} (pM^{-1}/h)	Second-order binding rate constant for free receptors and drug molecules	0.12
k_{off} (h^{-1})	First-order dissociation rate constant for drug-receptor complexes	18.0
k_{int} (h^{-1})	First-order internalization rate constant for bound receptors	6.0
ξ [$pM/(10^9 \text{ receptor})$]	Scaling factor converting the units of cell cellular concentration to nanomolar amounts	0.00166 ^a
I_{max}	Maximal inhibitory effect	1 (IDR 1, IDR 2)
S_{max}	Maximal stimulatory effect	2 (IDR 3) 5 (IDR 4)
Ib_{50} (receptors/cell)	Number of bound receptor per cell eliciting half of the maximal inhibitory effect	50 (IDR 1), 25 (IDR 2)
Sb_{50} (receptors/cell)	Number of bound receptor per cell eliciting half of the maximal stimulatory effect	50 (IDR 3, IDR 4)

N_A Avogadro's number

^a $\xi = 10^9/(10^{-12} N_A)$

associated with a single dose of filgrastim. Sixteen subjects received a single IV infusion of 375 mg over 25 min followed by a 14 day washout period, then followed by the administration of a SC dose of 375 mg. Collected data included 454 G-CSF serum concentrations and 416 ANC measures. In Study 91770, the PDMDD effects of repeated dosing was characterized by a cohort (n = 4) of subjects receiving 300 mg of filgrastim SC QD for 10 days. Pre-dose samples were taken each day and intensive sampling was performed on days 0 and 9. A total of 102 serum G-CSF concentration records and 120 ANC measurements were available for the analysis.

Structural model

The structural model was based on a granulopoiesis model previously developed [26, 27], which was modified by incorporating cellular level expression of receptors as described in Fig. 1. The resulting system is shown in Fig. 2.

Subcutaneous absorption

The absorption of filgrastim from the subcutaneous injection site was modeled with first-order transport k_a and a lag time t_{lag} :

$$\frac{dA_{SC}}{dt} = \sum_{i=1}^m F \cdot Dose_{SC} \cdot \delta(t - t_i - t_{lag}) - k_a \cdot A_{SC} \quad \text{and} \\ A_{SC}(0) = 0, \tag{12}$$

where A_{SC} is the drug amount in the subcutaneous site to be absorbed by the first-order rate k_a with the bioavailability F . The injections at times t_i ($i = 1, \dots, m$) are described by the delta functions $Dose_{SC} \cdot \delta(t - t_i - t_{lag})$.

Disposition and receptor binding

First-order processes are used to characterize the distribution to (k_{pt}) and from (k_{tp}) the tissue space as well as systemic elimination (k_{el}) of the drug. Second-order association and first-order dissociation rate constants k_{on} and k_{off} are used to describe the interaction between the G-CSF and the cell surface receptors (G-CSFRs).

$$\frac{dA_P}{dt} = k_{end} + \sum_{i=1}^m Dose_{IV} \cdot \delta(t - t_i) + k_a \cdot A_{SC} - k_{pt} \cdot A_P \\ + k_{pt} \cdot A_T - k_{el} \cdot A_P - k_{on} \cdot A_P \cdot R + k_{off} \cdot B \cdot V_c \\ \text{and } A_P(0) = A_{P0}, \tag{13}$$

$$\frac{dA_T}{dt} = k_{pt} \cdot A_P - k_{tp} \cdot A_T \quad \text{and} \quad A_T(0) = A_{T0}, \tag{14}$$

where k_{end} is the constant production rate of the endogenous G-CSF, V_c is the volume of the plasma compartment, A_{P0} and A_{T0} are the endogenous G-CSF amounts in the plasma and peripheral compartments, respectively. R and B denote the plasma concentration of free and bound G-CSFRs.

The G-CSFR kinetics at the cellular level are described by Eqs. (5)–(6) with the baseline conditions (10) modified to account for non-zero bound receptors due to the presence of endogenous G-CSF:

$$r(0) = r_0 = \frac{k_{syn}}{k_{deg}}, \quad \text{and} \quad b(0) = b_0. \tag{15}$$

The G-CSFRs are expressed on the circulating neutrophils (N) and neutrophil precursors in the bone marrow (P_i , $i = 1, 2, 3, 4$). The concentration of free and bound receptors in the plasma and bone marrow can be calculated as

$$R = \xi \cdot r \cdot (P_1 + P_2 + P_3 + P_4 + N)/V_c, \tag{16}$$

$$B = \xi \cdot b \cdot (P_1 + P_2 + P_3 + P_4 + N)/V_c. \tag{17}$$

Here, we assumed that the plasma volume (V_c) represents the binding space for all of the drug and receptors present in the system (plasma and bone marrow). The constant ξ represents the receptor density in nanomole amounts (nmol)/cell count (10^9 cells).

G-CSF effect on granulopoiesis

The G-CSF stimulates proliferation and accelerates maturations of the neutrophil precursors in the bone marrow. The proliferating progenitors (P_1) are assumed to be produced at the zero-order rate k_{in} and transition to the maturing cells (P_2) at the first-order rate k_{tr} . The maturation process in the bone marrow is further modeled by additional P_3 and P_4 transit compartments with the same transit rate constant k_{tr} resulting in the production of the circulating neutrophils N :

$$\frac{dP_1}{dt} = k_{in} \cdot S_p(b) - k_{tr} \cdot S_m(b) \cdot P_1 \quad \text{and} \quad P_1(0) = P_{10}, \tag{18}$$

$$\frac{dP_2}{dt} = k_{tr} \cdot S_m(b) \cdot P_1 - k_{tr} \cdot S_m(b) \cdot P_2 \quad \text{and} \\ P_2(0) = P_{20}, \tag{19}$$

$$\frac{dP_3}{dt} = k_{tr} \cdot S_m(b) \cdot P_2 - k_{tr} \cdot S_m(b) \cdot P_3 \quad \text{and} \\ P_3(0) = P_{30}, \tag{20}$$

$$\frac{dP_4}{dt} = k_{tr} \cdot S_m(b) \cdot P_3 - k_{tr} \cdot S_m(b) \cdot P_4 \quad \text{and} \\ P_4(0) = P_{40}. \tag{21}$$

The neutrophils undergo margination and diapedesing to the extravascular tissues, and are removed from the system at the first-order rate k_{out} :

$$\frac{dN}{dt} = k_{ir} \cdot S_m(b) \cdot P_4 - k_{out} \cdot N \quad \text{and} \quad N(0) = N_0. \quad (22)$$

All cellular responses are assumed to be at their baseline levels $P_{10}, P_{20}, P_{30}, P_{40}$ and N_0 prior to drug treatment. The stimulatory effects of G-CSF associated with cellular proliferation $[S_p(b)]$ and maturation $[S_m(b)]$ are described by the sigmoid functions of the number of bound receptor on a single cell

$$S_p(b) = 1 + \frac{S_{maxp} \cdot b^{\gamma_p}}{b_{50p}^{\gamma_p} + b^{\gamma_p}} \quad \text{and} \quad S_m(b) = 1 + \frac{S_{maxm} \cdot b^{\gamma_m}}{b_{50m}^{\gamma_m} + b^{\gamma_m}}, \quad (23)$$

where S_{maxp} and S_{maxm} are the maximal drug effects on proliferation and maturation processes, respectively, and b_{50p} and b_{50m} are the numbers of bound receptor/cell eliciting 50 % of the maximum drug effect on proliferation and maturation processes, respectively, and γ_p and γ_m are the Hill factors associated with drug effects on proliferation and maturation processes, respectively.

Baselines

The baseline relationships between model parameters and variables are obtained from the steady-state equations for differential equations (5)–(6), (13)–(14), and (18)–(22):

$$b_0 = \frac{k_{on} \cdot C_{p0}}{k_{off} + k_{int}} \cdot r_0, \quad (24)$$

$$k_{syn} = k_{deg} \cdot r_0 + k_{int} \cdot b_0, \quad (25)$$

$$A_{T0} = \frac{k_{pt}}{k_{tp}} \cdot A_{P0}, \quad (26)$$

$$P_{10} = P_{20} = P_{30} = P_{40} = N_0, \quad (27)$$

$$k_{end} = k_{el} \cdot A_0 + k_{int} \cdot b_0 \cdot \zeta(P_{10} + P_{20} + P_{30} + P_{40} + N_0), \quad (28)$$

$$k_{in} = \frac{k_{out} \cdot N_0}{S_p(b_0)}. \quad (29)$$

Reparameterization

The first-order elimination rate constant k_{el} was replaced by the clearance parameter:

$$k_{el} = CL \cdot V_c, \quad (30)$$

and, the transit rate constant k_{tr} by the mean transit time (MTT) in bone marrow:

$$k_{tr} = 4/MTT. \quad (31)$$

Additionally, the baseline ANC (ANC_0) and the endogenous G-CSF plasma concentration C_{P0} were used to calculate N_0 and A_0 :

$$N_0 = ANC_0 \cdot V_c \quad \text{and} \quad A_{P0} = C_{P0} \cdot V_c. \quad (32)$$

Results

The cell-level PDMDD model was studied by means of mathematical analysis, computer simulations, and fitting to clinical data. The major focus was on the comparison with the TMDD models with respect to the nonlinear concentration-dependent PK and quantifying the impact of the time-dependent change in the PD (the cell count) on the PK of the drug (nonlinear non-stationary PK). For that reason, one can consider the differential equations for the free (R) and bound (B) receptors present in the classic TMDD model [21]. These can be obtained by differentiation of (1) and substituting for the time derivatives of r, b, and N

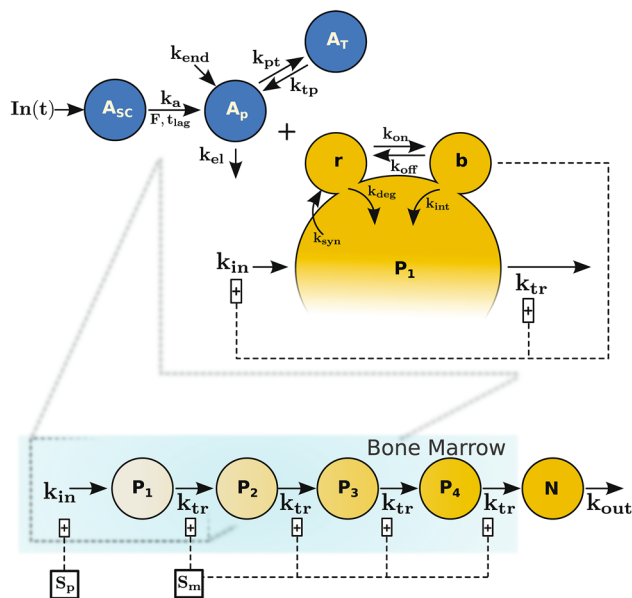


Fig. 2 Schematic diagram using the cell-level PDMDD model to describe the effects of filgrastim dosing on neutrophils. The general components and parameters are described in Fig. 1. In adapting the model five separate populations were considered: precursor cells (P_1) are produced at a rate k_{in} , mature at a rate k_{tr} through the catenary compartments (P_2 – P_4), and become measurable as neutrophils (N) which are eliminated at a rate k_{out} . Endogenous G-CSF is produced at a rate k_{end} . Filgrastim is administered into the subcutaneous compartment (A_{sc}) and is adsorbed into the plasma space at a rate k_a , with a lag time t_{lag} , and a bioavailability F . Bound receptors/cell (b) stimulate both the production (S_p) and maturation (S_m) of k_{in} and k_{tr} , respectively

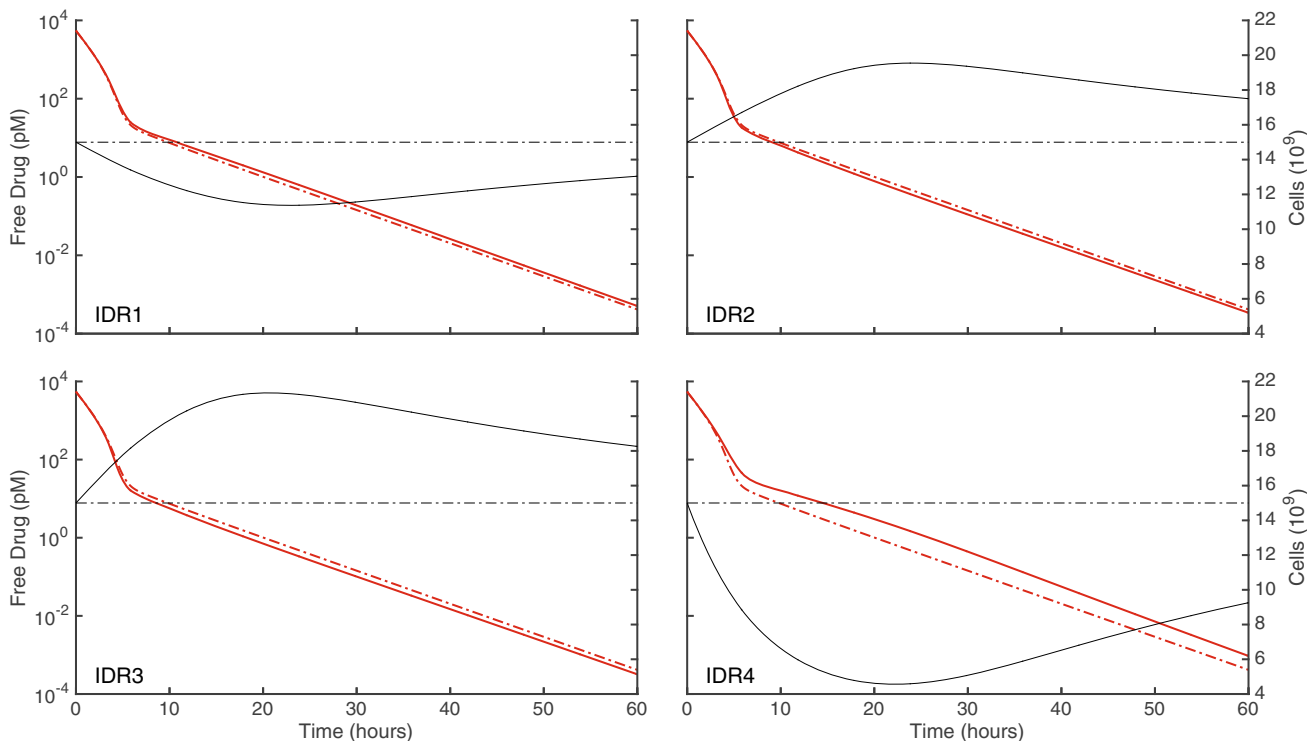


Fig. 3 Simulated time courses of free drug plasma concentrations $C(t)$ (thick, red) and cell counts $N(t)/V_c$ (thin, black) described by the models (2)–(10) following a single IV bolus dose of 10,000 pmol of drug for four types of the PD responses. The broken lines represent time courses where the cells are not affected by the drug treatment ($I_{max} = S_{max} = 0$)

$$\frac{dR}{dt} = \frac{\xi \cdot N}{V_c} \frac{dr}{dt} + \frac{\xi \cdot r}{V_c} \frac{dN}{dt} \quad \text{and} \quad \frac{dB}{dt} = \frac{\xi \cdot N}{V_c} \frac{db}{dt} + \frac{\xi \cdot b}{V_c} \frac{dN}{dt} \tag{33}$$

The immediate benefit of Eq. (33) is the ability to quantify the effect of the change of the cell population size (PD) on the receptor kinetics. Namely, the terms in Eq. (33) with the derivative dN/dt describe the contribution of the change of N to the change of R and B . The same rationale applies to quantifying the contribution of the change of the cell population size on the time course of the total receptors R_{tot} and the total drug C_{tot} . Consequently, after the relevant substitutions:

$$\frac{dR}{dt} = K_{syn} - k_{on} \cdot C \cdot R + k_{off} \cdot B - k_{deg} \cdot R + \frac{k_{in} \cdot \xi \cdot r}{V_c} \cdot (1 + H_{in}(b)) - k_{out} \cdot (1 + H_{out}(b)) \cdot R, \tag{34}$$

$$\frac{dB}{dt} = k_{on} \cdot C \cdot R - (k_{int} + k_{off}) \cdot B + \frac{k_{in} \cdot \xi \cdot b}{V_c} \cdot (1 + H_{in}(b)) - k_{out} \cdot (1 + H_{out}(b)) \cdot B, \tag{35}$$

where the synthesis rate for free receptors K_{syn} is the product of the synthesis rate of free receptors/cell $k_{syn} \cdot \xi$ and the concentration of cells in the central compartment N/V_c :

$$K_{syn} = \frac{k_{syn} \cdot \xi \cdot N}{V_c} \tag{36}$$

Absence of PD effect

If the drug does not affect the turnover of the cell population [$H_{in}(b) = H_{out}(b) = 0$], then the cell response remains constant and equal to the baseline:

$$N \equiv N_0 = \frac{k_{in}}{k_{out}} \tag{37}$$

Then (34) and (35) become identical with the differential equations in the classic TMDD model:

$$\frac{dR}{dt} = K_{syn} - k_{on} \cdot C \cdot R + k_{off} \cdot B - k_{deg} \cdot R, \tag{38}$$

$$\frac{dB}{dt} = k_{on} \cdot C \cdot R - (k_{int} + k_{off}) \cdot B, \tag{39}$$

where the synthesis rate of the free receptors K_{syn} is constant and equal to (36) with $N = N_0$. Reciprocally, by reducing the differential equations for R and B to the classic TMDD model with K_{syn} defined by (3), then (34) and (35) imply that $dN/dt = 0$, and the cell count must be constant. Consequently, the classic TMDD model is a subset of the PDMDD model presented here and represents

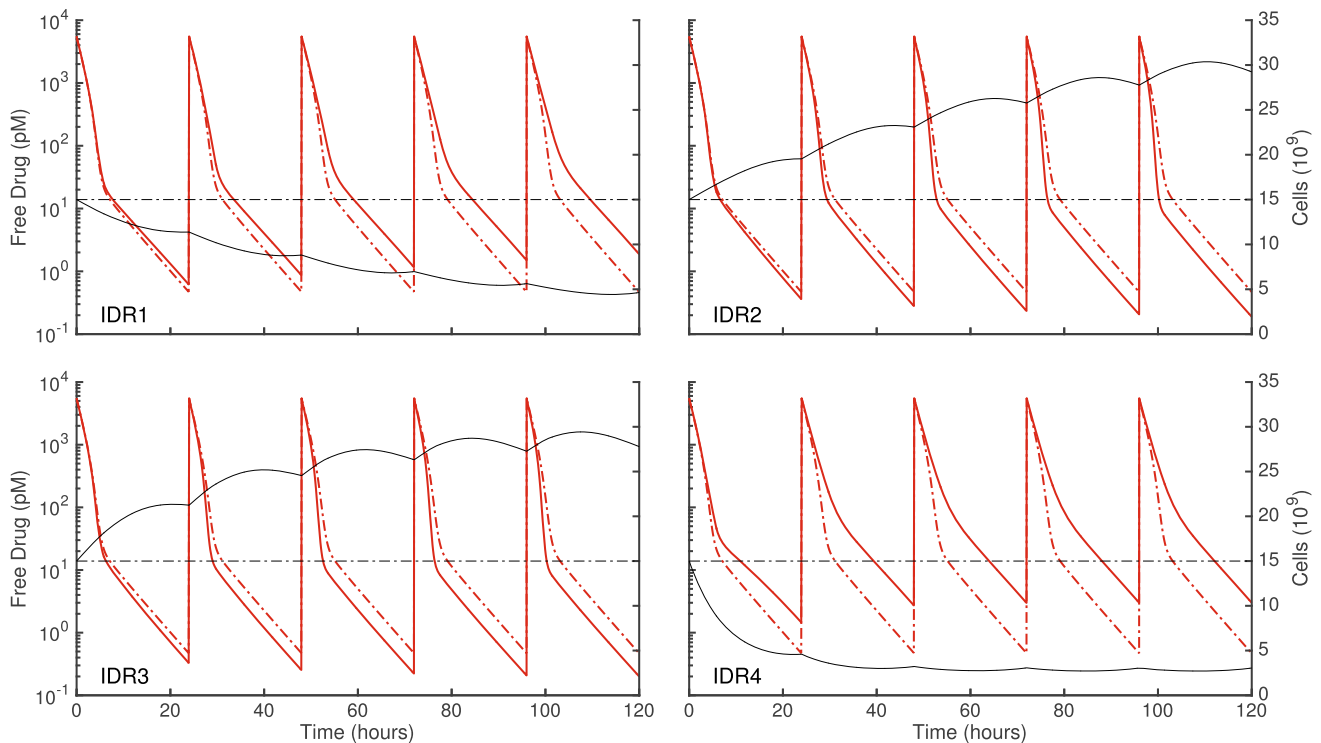


Fig. 4 Free drug plasma concentrations (*thick, red*) and corresponding cell count responses (*thin, black*) for QD IV bolus doses of 10,000 pmol for 5 days. The *continuous lines* correspond to the drug

effects on the cell counts described by models *IDR 1–4*, and the *broken lines* represent predictions where cell responses are not affected by the drug

the case where the drug does not alter the cell turnover and, subsequently, the target pool. This statement is true regardless the mathematical form for the stimulatory and inhibitory effects (8) and implies the absence of time-dependent PK.

Single dose

Figure 3 shows the mean predicted time courses of the free drug concentration in the central compartment in the absence of the PD effect superimposed with the predicted time courses altered by PD response described by all four models (8). A single dose of 10,000 pmol altered the cell counts by 24, 30, 42, and 70 % of the baseline values for models IDRs 1, 2, 3, and 4, respectively, however only a moderate change in the free drug concentration levels was predicted. In the predictions, the concentration increased when the cell-level decreased, and decreased with the increased cell response, consistent with the change in the total receptor pool size. These simulations show that the impact of the PD response on the receptor-mediated clearance following a single dose might not be substantial. Therefore the following series of simulations were performed to address the changes in the receptor-mediated

clearance after repeated doses where the PD response accumulates and reaches a new dynamic steady-state.

Repeated doses

A single dose PD response returns to the baseline after the drug clears from the system resulting in a transient PD impact on the disposition of the drug. After repeated dosing, a periodic PD response develops (defined by the dosing interval) with a trough cellular concentration that can be significantly different from the pre-dose baseline. This also implies that a complementary periodic shift will be seen in the free drug PK. Simulations of multiple dosing scenarios (Fig. 4) indicate that the time to reach a consistent periodic response for $N(t)$ and $C(t)$ coincide, because the receptor density is assumed to be constant over time. Additionally, upon repeated dosing, the predicted PD response increases and elicits larger effect on the clearance of drug than the loss due to cellular interactions after a single dose. When comparing the PK of subsequent doses in each model described in (8), the peak concentrations remain indistinguishable (due to the nadir being several orders of magnitude different from the peak), while the pre-dose troughs shift with time. As a result of the non-stationary PK profiles for the models differentiated by

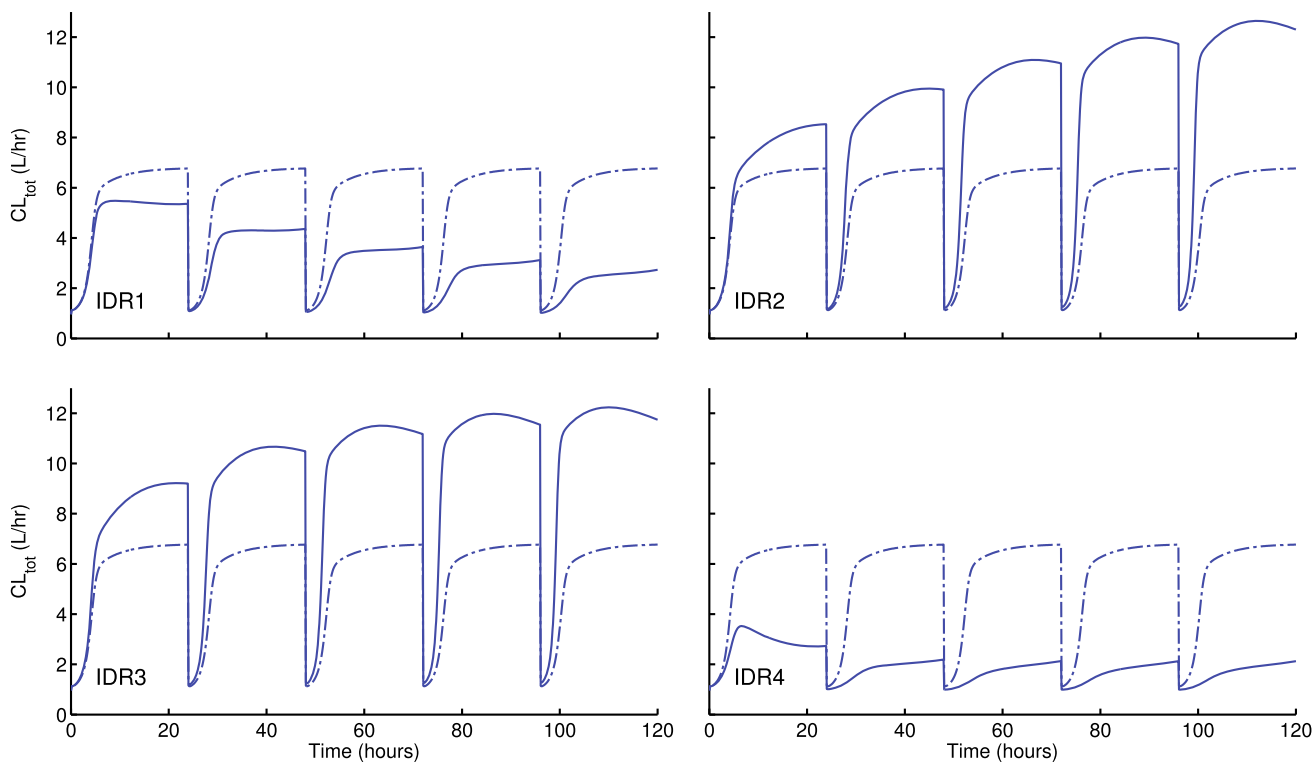


Fig. 5 Time courses of the total drug clearance for repeated doses of 10,000 pmol IV bolus QD for 5 days. The CL_{tot} was calculated using Eq. (40). The *continuous lines* correspond to the drug effects on the

cell counts described by models *IDR 1–4*, and the *broken lines* represent the clearance where cell responses are not affected by the drug

Table 2 Summary of observational statistics for single dose and multiple dose cohorts

	Single dose			
	G-CSF C_{max} (nM)	G-CSF t_{max} (h)	ANC $_{max}$ (10^9 cells/L)	t_{ANCmax} (h)
IV	10.6 ± 2.2	0.6 ± 0.2	25.9 ± 5.5	12
SC	1.6 ± 0.6	4.1 ± 0.5	26.2 ± 4.0	12
	Multiple dose			
	G-CSF C_{max} (nM)	G-CSF C_{24} (nM)	ANC $_{max}$ (10^9 cells/L)	AUC $_{0-24}$ (nM·h)
First dose	0.9 ± 0.4	0.01 ± 0.004	22.2 ± 6.3	7.4 ± 2.6
Tenth dose	0.2 ± 0.1	0.005 ± 0.001	48.1 ± 11.7	5.7 ± 1.5

Subjects given 375 mg of G-CSF as single an IV infusion (15 mg/min) and a single SC bolus dose, separated by a 14 day washout period and multiple dose cohorts (300 mg SC QD for 10 days). Data are presented as the mean ± standard deviation

Eq. (8), temporal changes in exposure are also predicted. When increasing the dosing interval, exposure (AUCs) increases for the IDR 1 and IDR 4 scenarios and decreases for the IDR 2 and IDR 3 scenarios. There was no change between AUC_{0-24} and AUC_{96-120} for the free drug plasma concentrations that did not affect cell counts (i.e., $S_{max} = I_{max} = 0$). However, the percent change between AUC_{0-24} and AUC_{96-120} were 21, -16, -15, and 26 % for

IDR 1, 2, 3, and 4, respectively. This implies that the PD effect significantly changes drug exposure and clearance upon multiple dosing, resulting in nonlinear time-dependent PK.

To quantify the total clearance of the drug from the body we combined the differential equations for C_{tot} and R_{tot} (“Appendix 1”) resulting in the following relationship:

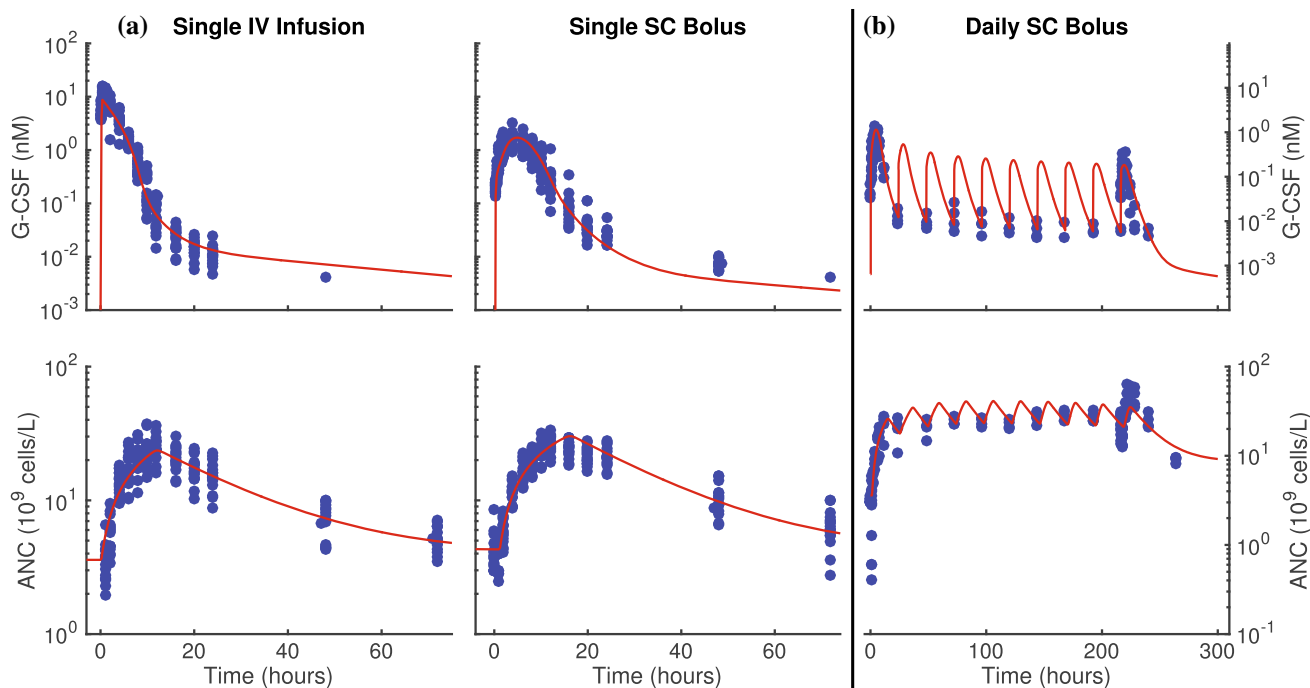


Fig. 6 Neupogen plasma concentrations and ANC (*symbols*) and model predicted values (*lines*) following administration of **a** single IV and SC doses of 375 μg and **b** repeated daily SC doses of 300 μg

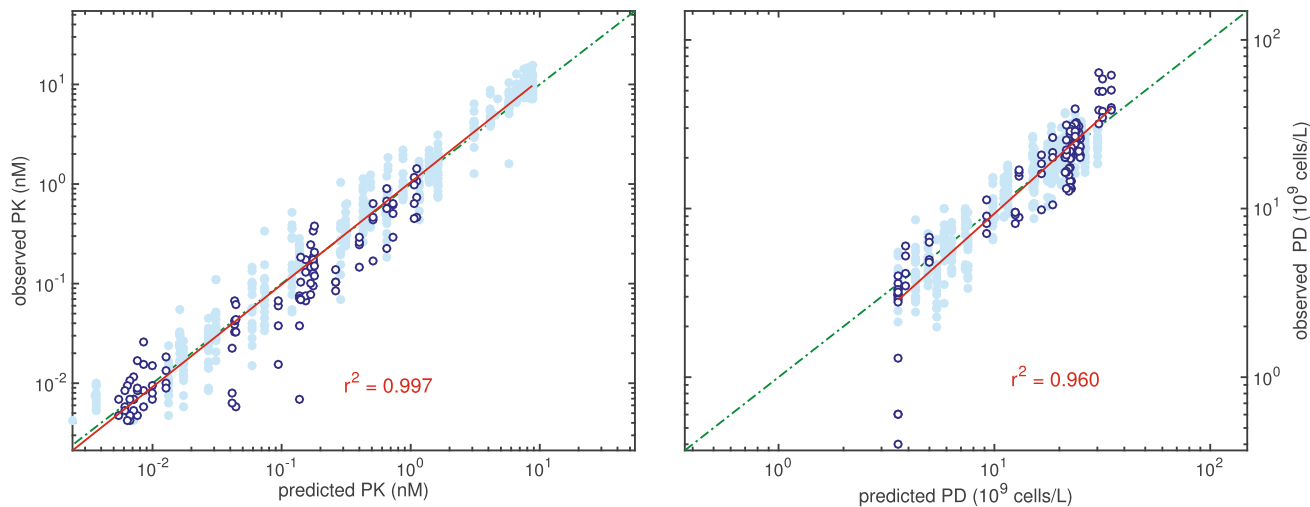


Fig. 7 Observed versus predicted time courses for PK (*left*) and PD (*right*): *dark open-circle* daily SC doses of 300 μg , *light solid-circle* single IV and SC doses of 375 μg , *dashed line* the line of identity, *solid line* least squares regression

$$\begin{aligned}
 CL_{\text{tot}} &= \frac{\text{elimination rate}}{C} \\
 &= k_{el} \cdot V_c + \frac{k_{\text{int}} \cdot V_c \cdot B}{C} + k_{\text{out}} \cdot (1 + H_{\text{out}}(b)) \frac{V_c \cdot B}{C}.
 \end{aligned}
 \quad (40)$$

For the different corresponding scenarios captured in Fig. 4, the time course of total clearance is shown in Fig. 5.

Case study

Summary information for typical metrics used to quantify PK/PD systems is shown in Table 2. In Study 930240, the single dose cohorts show the maximum G-CSF and ANC levels, and corresponding times, for the different routes of administration. Statistics for Study 91770 demonstrate the change in PK/PD measures with increasing dose. The

PDMDD model (13)–(22) was simultaneously fitted to G-CSF and ANC data obtained from two clinical studies in healthy volunteers. The data and fitted curves are shown in Fig. 6a, b and the observed versus predicted values are presented in Fig. 7.

The single dose study yielded G-CSF plasma concentrations that started at the pre-dose endogenous level that was below the limit of quantification, reached a peak and returned to the baseline. The rate of onset and offset was larger for the IV than SC plasma concentrations, and the time to reach the baseline was approximately 24 and 48 h following the dosing event, respectively. The corresponding ANC responses exhibited similar patterns with an increase from the baseline, reaching the peak, then gradually return to the baseline. The model adequately predicted the observed single dose data. The time courses of the predicted ANC peaked at 12 and 16 h for IV and SC routes, respectively. The multiple SC doses of 300 mg/kg QD resulted in gradual increases in the ANC values at trough PK sampling times. These corresponded to decreasing

G-CSF trough levels. The model accurately described the evolution of PDMDD for both PK and PD measures through the duration of the study with the predicted ANC and G-CSF trough levels reaching a new steady-state after four doses as shown in Fig. 6. The model slightly under-predicted the peaks of G-CSF and ANC after the 10th dose. The predicted G-CSF concentration and ANC time courses following the last dose returned to the baseline.

The parameter estimates are presented in Table 3. The model parameters were estimated with good precision ($\leq 24\%$ CV). The baseline value, ANC_0 , was fixed at the mean pre-dose measurement to reduce the number of model parameters. Difficulties with estimation of the remaining set of parameters were resolved by fixing the following parameters to the literature-reported values: $K_D = 0.045$ nM [28] and $k_{deg} = 0.215$ h⁻¹ [29]. Since the baseline G-CSF plasma concentration was below the limit of detection, it was fixed at the reported level of endogenous G-CSF for healthy humans $C_0 = 0.00064$ nM (11.94 pg/mL) [30]. The estimates of CL and V_c are very

Table 3 Parameter estimates for the PDMDD model of G-CSF effect on neutrophils

Parameter (unit)	Definition	Estimate	CV%
CL (L/h)	G-CSF plasma clearance	0.132	24.4
V_c (L)	Volume of the plasma compartment	1.75	3.4
k_{pt} (h ⁻¹)	First-order rate constant for G-CSF distribution to the tissue space	0.123	11.4
k_{ip} (h ⁻¹)	First-order rate constant for G-CSF distribution from the tissue space	0.0224	18.6
k_a (h ⁻¹)	Filgrastim first-order absorption rate constant	0.20	3.4
t_{lag} (h)	Filgrastim absorption lag time	0.225	1.7
F	Filgrastim bioavailability	1.0	FIX
C_{P0} (nM)	Endogenous G-CSF plasma concentration	0.00064	FIX
r_0 (receptors/cell)	Baseline free G-CSFR per cell	27,000	10.3
K_D (nM)	G-CSF equilibrium disassociation constant	0.045	FIX
k_{off} (h ⁻¹)	Second-order binding rate constant for free G-CSFR and G-CSF	0.107	10.7
k_{deg} (h ⁻¹)	First-order dissociation rate constant for bound G-CSFR	0.215	FIX
k_{int} (h ⁻¹)	First-order internalization rate constant for bound G-CSFR	0.189	6.3
ξ (nmol/receptor)	Scaling factor converting the units of cell cellular concentration to nanomolar amounts	0.00000166 ^a	FIX
k_{out} (h ⁻¹)	Neutrophil first-order elimination rate constant	0.0480	5.3
MTT (h)	Mean transit time for neutrophil maturing precursors	267	11.2
ANC_0 (10 ⁹ cells/L)	Baseline absolute neutrophil count	3.59	FIX
S_{maxp}	Maximal G-CSF effect on proliferation process	14.2	6.8
S_{maxm}	Maximal G-CSF effect on maturation process	13.1	5.3
Sb_{50p} (receptors/cell)	Number of bound G-CSFR per cell eliciting half of the maximal stimulatory effect on cell proliferation	7190	15.7
Sb_{50m} (receptors/cell)	Number of bound G-CSFR per cell eliciting half of the maximal stimulatory effect on cell maturation	14,400	8.9
γ_p	Hill factor associated with G-CSF effect on cell proliferation	20	FIX
γ_m	Hill factor associated with G-CSF effect on cell maturation	20	FIX

N_A Avogadro's number

^a $\xi = 10^9/(10^{-9} N_A)$

similar to the ones reported previously [14]. Compared to previous estimates of the distribution parameters, current estimates of k_{ip} and k_{pr} are 5-fold smaller and 8-fold larger, respectively [14]. Due to approaching boundary during estimation, the bioavailability F was fixed at 1. Addition of the absorption lag time significantly improved the fittings, but the estimated value of t_{lag} was small relative to the observed t_{max} . The estimated absorption rate constant k_a was similar to the absorption rates in the dual absorption model [14] and the dissociation rate constant, k_{off} , was about 10-fold smaller than previous reports [19], but similar to an estimate obtained by a TMDD model for filgrastim previously reported [29]. The estimated number of G-CSFR/cell is about 54-fold larger than the value of 50–500 reported in the literature [31]. Such a high number is necessary to eliminate rHu-G-CSF by the receptor-mediated endocytosis and loss of neutrophils. This over-estimate might compensate for G-CSFR pools that were not included into the model. The mean residence time for the circulating neutrophils calculated as $1/k_{out} = 20.8$ h is close to the circulating neutrophil lifespan 10 h [32]. The estimate of the MTT in the bone marrow (11.1 days) was consistent with the literature reported values of 8–15 days [32]. The estimates of the maximal stimulation of the proliferation precursor S_{maxp} and acceleration of the maturation S_{maxm} were similar and they resulted in a little more than 10-fold increase for large doses. A 2.4-fold difference was observed between Sb_{50m} and Sb_{50p} indicating that G-CSF is more potent when stimulating the proliferation than accelerating the maturation of the neutrophils precursors, consistent with previous analysis [33].

Discussion

Typically, TMDD effects can be detected from single ascending dose data by observing the change in the steady-state volume of distribution and clearance (via non-compartmental analysis) with changing dose levels [21]. Our simulations show that multiple doses may be required in order for the cellular response to fully develop such that its contribution to the target-mediated disposition is maximally observable. Therefore in order to detect the presence of PDMDD from PK data alone, a repeated dosing study is recommended. The change in clearance between the doses is a strong indication of the impact of PD on the drug disposition. In this case, non-compartmental assessment of the change in clearance involves calculation of AUC for the dosing time intervals and observing the change following consecutive doses. If PK is linear such AUCs will be equal [34]. Since changes in AUC values might be caused by factors not related to cellular response, it is recommended that the selection of time spans of the AUC

values be related to the time course of PD in order to establish a causal relationship.

Existing approaches to account for PDMDD applied rather crude assumptions about the relationship between the pool of receptors and the cell count. In essence, the concentration of the total receptors is assumed to be proportional to the number of cells expressing them [2, 14]. This may bias the TMDD model by neglecting the turnover of the receptors (production and degradation). More importantly, it is very difficult to quantify the drug clearance resulting from receptor binding, since one would have to calculate the elimination rate of the drug–receptor complexes, which are removed with the cells. Including the cell-level model of drug–target binding alleviates both of these limitations. Expressing the pool of receptors as the product of receptors/cell and the cell number allows one to describe the receptor turnover as well as precisely quantify the contribution of internalization and changes in cell number to the overall drug clearance. The assumption that target expression is same for all cells is less restrictive and can be justified by averaging the receptor number/cell over the cell population and using it as an approximation of the actual number. In this formulation, the cell-level PDMDD model offers more mechanistic description of the receptor pool dynamics. However, to fully characterize the heterogeneity of the receptor distribution among cells requires additional mathematical tools, such as physiologically structured population models [35], to be further investigated.

The introduced cell-level PDMDD model has exactly the same set of binding parameters as the standard TMDD model (a subset of the PDMDD model). The primary difference is that parameters associated with the target synthesis and maintenance (k_{syn} and r_0) have units of numbers/cell rather than the absolute number or concentration. Therefore, the issue of the parameter identifiability is the same as for the standard TMDD model with the additional problem of the identifiability of the some PD model parameters. Based on available PK data, further simplifications of the TMDD model have been introduced to reduce the number of model parameters [16]. Analogous simplifications can be proposed of the cell-level receptor binding model with almost no modification. In “Appendix 2”, we provide the rapid binding approximation [16] of the cell-level model that is valid under the assumption that the binding and dissociation of the drug to the target are faster than all other processes described by the model. Consequently, one can replace the binding parameters k_{on} and k_{off} with a single equilibrium dissociation parameter K_D , reducing the model dimensionality by one.

The PD model being an intrinsic part of the PK model of TMDD is the key feature of the PDMDD model. This implies that it is necessary to analyze both PD and PK data

jointly in order to characterize the system. This is an important difference between PDMDD and TMDD models where the latter can be successfully identified from PK data alone. Absence of PD data in analysis of systems exhibiting PDMDD can manifest in presence of the time-varying covariates accounting for time-varying drug clearance [36]. One can also erroneously attribute the time-varying clearance to between-occasion variability, particularly when this variability is not random with time. For compounds where PDMDD is expected to impact development, studies can be designed to characterize these properties (e.g., multiple doses and measures to quantify the PD evolution). However because of sampling limitations it may not be possible to quantify changes in the affected cellular populations. In these settings it may only be possible to analyze the system using a more traditional TMDD or Michaelis–Menten model, with empirical time dependent functions, and accept the limitations of these model predictions.

G-CSF and neutrophils are a well-documented system for studying PDMDD. Therefore, we selected G-CSF serum concentrations and ANC in healthy subjects as data sets to test the PDMDD model. The model adequately described the data and the estimated parameter values were within the physiological ranges or agreed with similar parameters reported in the literature. In addition to explaining the neutrophil-mediated disposition of G-CSF, the model described the kinetics of the eG-CSF. The PDMDD of eG-CSF has been suggested as a feedback mechanism underlying the rebound in ANC following chemotherapy induced neutropenia in cancer patients [4, 37]. Although tuned for the stimulatory effect of G-CSF, the presented PDMDD model is capable of quantifying the rebound effect in ANC due to accumulation eG-CSF in neutropenic patients. eG-CSF serum concentrations and ANC in cancer patients with chemotherapy induced neutropenia would be another data set to test the utility of the cell-level PDMDD model.

Identification of appropriate dose and dosing schedule can be challenging for drugs that exhibit PDMDD, since it leads to a time- and concentration-dependent clearance and results in a complex interaction between drug PK and target dynamics. Daratumumab, a CD38 IgG1k monoclonal antibody recently approved to relapsed and refractory multiple myeloma patients, exhibits PDMDD since it is expected to have slower clearance over time due to the drug-induced depletion of the CD38 cells, as well as slower clearance at higher drug concentrations when the target becomes saturated [38]. The currently approved dose regimen of daratumumab manages to provide rapidly maximal efficacy with weekly administration of 16 mg/kg for eight consecutive weeks and then maintain an exposure range that warrants target saturation thereafter, thus reducing the risk of disease progression at the less frequent biweekly

(for 16 weeks) and monthly administration. Although the concentration of daratumumab tended to decrease following the biweekly and monthly dosing until reaching steady state, the reduction in concentration over time observed in clinical studies was not associated with higher risk of disease progression. Furthermore, lowering the dose below 16 mg/kg would likely result in reduced efficacy because the reduction on target occupancy, whereas increasing the dose would not provide further improvement of the benefit–risk profile [39]. The modeling approach described in this paper provides a framework that could be applied to the assessment of the dose selection for other mAbs in clinical development that exhibit PDMDD, such as obinutuzumab [40].

Conclusion

Four types of PDMDD models were studied for their impact on PK following single and repeated dosing. Our major finding was that a single dose might not be sufficient to elicit the cellular response capable of altering the receptor pool to visibly affect drug plasma concentrations. We demonstrated that repeated dosing as a means of detecting and quantifying PDMDD may be necessary and consequently should be considered when designing studies where PDMDD is expected. The model equations provided mathematical relationships partitioning the drug clearance into linear, endocytotic internalization and degradation, and cell elimination. The TMDD model was shown to be a subset of the PDMDD model when the pharmacological effect does not significantly impact the number of target expressing cells in the system. The model was applied to describe the relationship between G-CSF concentration and ANC in healthy subjects receiving single and repeated doses of filgrastim. Among several other utilizations, future applications of this cell-level model may include chemotherapy induced cytopenias affecting clearance of endogenous hematopoietic growth factors, different monoclonal antibodies and immunogenicity effects on PK.

Compliance with ethical standards

Conflicts of interest The following authors are or were employees of and own stock in Amgen, Inc.: Juan Jose Perez-Ruixo, Liviawati S. Wu, and John M. Harrold. Wojciech Krzyzanski is a consultant for Amgen and received consultation fees for this work.

Appendix 1: Clearance of total drug

Since $A_{tot} = A_p + BV_c$ one can combine Eqs. (2) and (35) to obtain a differential equation

$$\frac{dA_{tot}}{dt} = In(t) - (k_{el} + k_{pt})A_P + k_{ip} \cdot A_T - k_{int} \cdot B \cdot V_c + k_{in} \cdot \xi \cdot b(1 + H_{in}(b)) - k_{out} \cdot (1 + H_{out}(b))B \cdot V_c. \quad (41)$$

Therefore the elimination rate of the total drug from the body is

$$\text{elimination rate} = k_{el} \cdot A_P + k_{int} \cdot B \cdot V_c + k_{out}(1 + H_{out}(b))B \cdot V_c. \quad (42)$$

Dividing (42) by C yields (40).

Appendix 2: Rapid binding approximation

In many instances receptor binding and dissociation are much faster than the remaining processes described by the model. This results in the inability to uniquely identify the binding parameters. To resolve this problem the rapid binding approximation of the full model (2)–(8) can be applied based on the quasi-equilibrium assumption [16]:

$$\frac{C \cdot r}{b} = \frac{k_{on}}{k_{off}} = K_D. \quad (43)$$

To be able to eliminate the binding parameters k_{on} and k_{off} from the model equations new variables are introduced, the total receptor number/cell (r_{tot}) and total amount of the drug in the central compartment (A_{tot}):

$$r_{tot} = r + b \quad \text{and} \quad A_{tot} = A_P + \xi \cdot b \cdot N. \quad (44)$$

Then the model equations become:

$$\frac{dA_{tot}}{dt} = In(t) - (k_{el} + k_{pt})C \cdot V_c + k_{ip} \cdot A_T - k_{int} \cdot \xi \cdot b \cdot N + \xi \cdot b \cdot \frac{dN}{dt}, \quad (45)$$

$$\frac{dA_T}{dt} = k_{pt} \cdot C \cdot V_c - k_{ip} \cdot A_T, \quad (46)$$

$$\frac{dr_{tot}}{dt} = k_{syn} - k_{deg} \cdot r_{tot} + (k_{deg} - k_{int}) \cdot b, \quad (47)$$

where the derivative dN/dt is defined by (7),

$$b = \frac{r_{tot} \cdot C}{K_D + C}, \quad (48)$$

and

$$C = \frac{1}{2} \left(C_{tot} - R_{tot} - K_D + \sqrt{(C_{tot} - R_{tot} - K_D)^2 + 4 \cdot K_D \cdot C_{tot}} \right). \quad (49)$$

The total drug and total receptor concentrations in the central compartment are defined as follows

$$C_{tot} = \frac{A_{tot}}{V_c} = C + B \quad \text{and} \quad R_{tot} = \frac{r_{tot} \cdot \xi \cdot N}{V_c} = R + B. \quad (50)$$

Given that $In(t)$ describes the input rate to the A_{tot} compartments (including bolus doses), the initial conditions for (45)–(47) are

$$A_{tot}(0) = 0, \quad A_T(0) = 0, \quad r_{tot}(0) = \frac{k_{syn}}{k_{deg}}, \quad N(0) = \frac{k_{in}}{k_{out}}. \quad (51)$$

References

- Levy G (1994) Pharmacologic target-mediated drug disposition. *Clin Pharmacol Ther* 56:248–252
- Wang Y-MC, Krzyzanski W, Doshi S et al (2010) Pharmacodynamics-mediated drug disposition (PDMDD) and precursor pool lifespan model for single dose of romiplostim in healthy subjects. *AAPS J* 12:729–740. doi:10.1208/s12248-010-9234-9
- Roskos LK (2012) The clinical pharmacology of filgrastim and pegfilgrastim. In: Twenty years of G-CSF. Springer, Basel, p 41–60
- Quartino AL, Karlsson MO, Lindman H, Friberg LE (2014) Characterization of endogenous G-CSF and the inverse correlation to chemotherapy-induced neutropenia in patients with breast cancer using population modeling. *Pharm Res* 31:3390–3403. doi:10.1007/s11095-014-1429-9
- Farese AM, Cohen MV, Stead RB et al (2012) Pegfilgrastim administered in an abbreviated schedule, significantly improved neutrophil recovery after high-dose radiation-induced myelosuppression in rhesus macaques. *Radiat Res* 178:403–413. doi:10.1667/RR2900.1
- Wang B, Nichol JL, Sullivan JT (2004) Pharmacodynamics and pharmacokinetics of AMG 531, a novel thrombopoietin receptor ligand. *Clin Pharmacol Ther* 76:628–638. doi:10.1016/j.clpt.2004.08.010
- Krzyzanski W, Sutjandra L, Perez-Ruixo JJ et al (2013) Pharmacokinetic and pharmacodynamic modeling of romiplostim in animals. *Pharm Res* 30:655–669. doi:10.1007/s11095-012-0894-2
- Bernstein SH, Jusko WJ, Krzyzanski W et al (2002) Pharmacodynamic modeling of thrombopoietin, platelet, and megakaryocyte dynamics in patients with acute myeloid leukemia undergoing dose intensive chemotherapy. *J Clin Pharmacol* 42:501–511. doi:10.1177/00912700222011553
- Yan X, Lowe PJ, Fink M, Berghout A (2012) Population pharmacokinetic and pharmacodynamic model-based comparability assessment of a recombinant human epoetin alfa and the biosimilar HX575. *J Clin Pharmacol*. doi:10.1177/0091270011421911/pdf
- Doshi S, Krzyzanski W, Yue S et al (2013) Clinical pharmacokinetics and pharmacodynamics of erythropoiesis-stimulating agents. *Clin Pharmacokinet* 52:1063–1083. doi:10.1007/s40262-013-0098-x
- Mould DR, Baumann A, Kuhlmann J et al (2007) Population pharmacokinetics–pharmacodynamics of alemtuzumab (Campath) in patients with chronic lymphocytic leukaemia and its link to treatment response. *Br J Clin Pharmacol* 64:278–291. doi:10.1111/j.1365-2125.2007.02914.x
- Gibiansky L, Frey N (2012) Linking interleukin-6 receptor blockade with tocilizumab and its hematological effects using a modeling approach. *J Pharmacokinet Pharmacodyn* 39:5–16. doi:10.1007/s10928-011-9227-z

13. Perez-Ruixo JJ, Ma P, Chow AT (2013) The utility of modeling and simulation approaches to evaluate immunogenicity effect on the therapeutic protein pharmacokinetics. *AAPS J* 15:172–182. doi:[10.1208/s12248-012-9424-8](https://doi.org/10.1208/s12248-012-9424-8)
14. Wang B, Ludden TM, Cheung EN et al (2001) Population pharmacokinetic–pharmacodynamic modeling of filgrastim (r-metHuG-CSF) in healthy volunteers. *J Pharmacokinet Pharmacodyn* 28:321–342. doi:[10.1023/A:1011534529622](https://doi.org/10.1023/A:1011534529622)
15. Krzyzanski W, Wiczling P, Lowe P et al (2010) Population modeling of filgrastim PK–PD in healthy adults following intravenous and subcutaneous administrations. *J Clin Pharmacol* 50:101S–112S. doi:[10.1177/0091270010376966](https://doi.org/10.1177/0091270010376966)
16. Mager DE, Krzyzanski W (2005) Quasi-equilibrium pharmacokinetic model for drugs exhibiting target-mediated drug disposition. *Pharm Res* 22:1589–1596. doi:[10.1007/s11095-005-6650-0](https://doi.org/10.1007/s11095-005-6650-0)
17. Gibiansky L, Gibiansky E, Kakkar T, Ma P (2008) Approximations of the target-mediated drug disposition model and identifiability of model parameters. *J Pharmacokinet Pharmacodyn* 35:573–591. doi:[10.1007/s10928-008-9102-8](https://doi.org/10.1007/s10928-008-9102-8)
18. Gross AW, Lodish HF (2006) Cellular trafficking and degradation of erythropoietin and novel erythropoiesis stimulating protein (NESP). *J Biol Chem* 281:2024–2032. doi:[10.1074/jbc.M510493200](https://doi.org/10.1074/jbc.M510493200)
19. Sarkar CA, Lauffenburger DA (2003) Cell-level pharmacokinetic model of granulocyte colony-stimulating factor: implications for ligand lifetime and potency in vivo. *Mol Pharmacol* 63:147–158. doi:[10.1124/mol.63.1.147](https://doi.org/10.1124/mol.63.1.147)
20. Krippendorff B-F, Oyarzún DA, Huisinga W (2012) Predicting the F(ab)-mediated effect of monoclonal antibodies in vivo by combining cell-level kinetic and pharmacokinetic modelling. *J Pharmacokinet Pharmacodyn* 39:125–139. doi:[10.1007/s10928-012-9243-7](https://doi.org/10.1007/s10928-012-9243-7)
21. Mager DE, Jusko WJ (2001) General pharmacokinetic model for drugs exhibiting target-mediated drug disposition. *J Pharmacokinet Pharmacodyn* 28:507–532
22. Shankaran H, Resat H, Wiley HS (2007) Cell surface receptors for signal transduction and ligand transport: a design principles study. *PLoS Comput Biol* 3:e101. doi:[10.1371/journal.pcbi.0030101](https://doi.org/10.1371/journal.pcbi.0030101)
23. Dayneka NL, Garg V, Jusko WJ (1993) Comparison of four basic models of indirect pharmacodynamic responses. *J Pharmacokinet Biopharm* 21:457–478. doi:[10.1007/BF01061691](https://doi.org/10.1007/BF01061691)
24. Harrold JM, Abraham AK (2014) Ubiquity: a framework for physiological/mechanism-based pharmacokinetic/pharmacodynamic model development and deployment. *J Pharmacokinet Pharmacodyn* 41:151. doi:[10.1007/s10928-014-9352-6](https://doi.org/10.1007/s10928-014-9352-6)
25. Borleffs JC, Bosschaert M, Vrethen HM et al (1998) Effect of escalating doses of recombinant human granulocyte colony-stimulating factor (filgrastim) on circulating neutrophils in healthy subjects. *Clin Ther* 20:722–736
26. Friberg LE, Freijs A, Sandström M, Karlsson MO (2000) Semi-physiological model for the time course of leukocytes after varying schedules of 5-fluorouracil in rats. *J Pharmacol Exp Ther* 295:734–740
27. Friberg LE, Karlsson MO (2003) Mechanistic models for myelosuppression. *Investig N Drugs*. doi:[10.1023/A:1023573429626](https://doi.org/10.1023/A:1023573429626)
28. Layton JE, Shimamoto G, Osslund T et al (1999) Interaction of granulocyte colony-stimulating factor (G-CSF) with its receptor. Evidence that Glu19 of G-CSF interacts with Arg288 of the receptor. *J Biol Chem* 274:17445–17451
29. Wiczling P, Lowe P, Pigeolet E et al (2009) Population pharmacokinetic modelling of filgrastim in healthy adults following intravenous and subcutaneous administrations. *Clin Pharmacokinet* 48:817–826. doi:[10.2165/11318090-000000000-00000](https://doi.org/10.2165/11318090-000000000-00000)
30. Kavgaci H, Ozdemir F, Aydin F et al (2002) Endogenous granulocyte colony-stimulating factor (G-CSF) levels in chemotherapy-induced neutropenia and in neutropenia related with primary diseases. *J Exp Clin Cancer Res* 21:475–479
31. Demetri GD, Griffin JD (1991) Granulocyte colony-stimulating factor and its receptor. *Blood* 78:2791–2808
32. McKenzie SB, Williams JL, Landis-Piwowar K (2014) *Clinical laboratory hematology*. Prentice Hall, Upper Saddle River
33. Ramon-Lopez A, Nalda-Molina R, Valenzuela B, Perez-Ruixo JJ (2009) Semi-mechanistic model for neutropenia after high dose of chemotherapy in breast cancer patients. *Pharm Res* 26:1952–1962. doi:[10.1007/s11095-009-9910-6](https://doi.org/10.1007/s11095-009-9910-6)
34. Gibaldi M, Perrier D (1982) *Pharmacokinetics*. Informa Health-Care, New York
35. Diekmann O, Gyllenberg M, Metz J (2007) Physiologically structured population models: towards a general mathematical theory. In: Takeuchi Y, Iwasa Y, Sato K (eds) *Mathematics for ecology and environmental sciences*. Springer, Berlin, pp 5–20
36. Ait-Oudhia S, Vermeulen A, Krzyzanski W (2011) Non-linear mixed effect modeling of the time-variant disposition of erythropoietin in anemic cancer patients. *Biopharm Drug Dispos* 32:1–15. doi:[10.1002/bdd.733](https://doi.org/10.1002/bdd.733)
37. Pastor ML, Laffont CM, Gladiéff L et al (2013) Model-based approach to describe G-CSF effects in carboplatin-treated cancer patients. *Pharm Res* 30:2795–2807. doi:[10.1007/s11095-013-1099-z](https://doi.org/10.1007/s11095-013-1099-z)
38. Yan X, Clemens PL, Puchalski T et al (2015) Target-mediated drug disposition of daratumumab following intravenous infusion in relapsed or refractory multiple myeloma after prior proteasome inhibitors and immunomodulatory drugs: a population pharmacokinetic analysis. *Blood* 126:4222
39. Xu XS, Yan X, Puchalski T et al (2015) Understanding the dose regimen for daratumumab in patients with relapsed or refractory multiple myeloma (MM) after prior proteasome inhibitors (PIs) and immunomodulatory drugs (IMiDs): a quantitative pharmacologic perspective. *Blood* 126:4254
40. Gibiansky E, Gibiansky L, Carlile DJ et al (2014) Population pharmacokinetics of obinutuzumab (GA101) in chronic lymphocytic leukemia (CLL) and non-Hodgkin’s lymphoma and exposure-response in CLL. *CPT Pharmacomet Syst Pharmacol* 3:1–11. doi:[10.1038/psp.2014.42](https://doi.org/10.1038/psp.2014.42)